Since January 2020 Elsevier has created a COVID-19 resource centre with free information in English and Mandarin on the novel coronavirus COVID-19. The COVID-19 resource centre is hosted on Elsevier Connect, the company's public news and information website.

Virology 433 (2012) 226–235

Contents lists available at SciVerse ScienceDirect

Virology

journal homepage: www.elsevier.com/locate/yviro

The helicase activity of DDX56 is required for its role in assembly of infectious West Nile virus particles

Zaikun Xu [a], Tom C. Hobman [a,b,c,*]

[a] Department of Cell Biology, University of Alberta, 5-14 Medical Sciences Building, Edmonton, Canada T6G 2H7
[b] Department of Medical Microbiology and Immunology, University of Alberta, Canada T6G 2H7
[c] Li Ka Shing Institute of Virology, University of Alberta, Canada T6G 2H7

ARTICLE INFO

Article history:
Received 26 April 2012
Returned to author for revisions
1 June 2012
Accepted 3 August 2012
Available online 25 August 2012

Keywords:
West Nile virus
Flavivirus
Helicase
DDX56
Nucleolus
RNA replication
Virus assembly
Microscopy
Capsid

ABSTRACT

Although flaviviruses encode their own helicases, evidence suggests that cellular helicases are also required for replication and/or assembly of these viruses. By and large, the mechanisms of action for viral and cellular helicases are not known. Moreover, in some cases, enzymatic activity is not even required for their roles in virus biology. Recently, we showed that expression of the host nucleolar helicase DDX56 is important for infectivity of West Nile virus (WNV) particles. In the present study, we demonstrate that the helicase activity of this enzyme is essential for its role in assembly of infectious WNV virions. Over-expression of the capsid-binding region of DDX56 also reduces infectivity of WNV suggesting that interaction of DDX56 and capsid protein is an important step in the virion assembly pathway. To our knowledge, this is the first study showing that enzymatic activity of a cellular helicase is critical for infectivity of flaviviruses.

Introduction

West Nile virus (WNV) is an important human pathogen that can cause severe neurological disease (reviewed in Brinton, 2002). It is wide spread throughout the globe and is maintained in an enzootic cycle with birds serving as the main reservoir. Similar to most other flaviviruses, mosquito-borne transmission is the main mode of human infection. Currently, there are no WNV-specific vaccines or therapies that are approved for use in humans.

As with all viruses, WNV is an obligate intracellular parasite that is completely dependent upon the host cell for viral entry, replication, assembly and egress. A recent study revealed that more than 300 human genes are required for replication of WNV and the closely related flavivirus, Dengue virus (Krishnan et al., 2008). In addition to replication, we anticipate that many other human genes are needed for assembly and secretion of nascent WNV virions. Rather than conducting genome-wide screens to identify host factors that are involved in WNV biology, we focused on cellular proteins that interact with the capsid protein. In addition to performing a critical structural role in virus assembly, our data indicate that interactions between this viral protein and the milieu of host proteins may contribute to pathogenesis (Hunt et al., 2007; van Marle et al., 2007). As well as potentially functioning in a negative capacity at the virus-host interface, interaction of WNV capsid with host proteins may be required for replication and/or virus assembly. With respect to the latter, we recently identified the nucleolar helicase DDX56 as a WNV capsid-binding protein (Xu et al., 2011).

Expression of DDX56 is not required for virus replication and thus could not have been identified in an RNAi screen designed to identify host factors that function in this process. However, expression of the nucleolar helicase DDX56 is important for infectivity of WNV virions (Xu et al., 2011). Findings from other laboratories indicate that both cellular and viral helicases play critical roles in the biology of flaviviruses (Ariumi et al., 2007; Krishnan et al., 2008; Mamiya and Worman, 1999; Owsianka and Patel, 1999; You et al., 1999). Accordingly, considerable efforts have been directed toward determining the feasibility of targeting cellular and viral helicases as a means to block viral infections (Geiss et al., 2009; Kwong et al., 2005; Maga et al., 2011; Stankiewicz-Drogon et al., 2010).

To aid in development of anti-viral therapies that target RNA helicases which are integral to flavivirus biology, it is critical to

* Corresponding author at: Department of Cell Biology University of Alberta, 5-14 Medical Sciences Building, Edmonton, Canada T6G 2H7.
Fax: +1 780 492 0450.
E-mail address: tom.hobman@ualberta.ca (T.C. Hobman).

0042-6822/$ - see front matter Crown Copyright © 2012 Published by Elsevier Inc. All rights reserved.
http://dx.doi.org/10.1016/j.virol.2012.08.011

understand how these enzymes function in this capacity. Indeed, evidence suggests that some RNA helicases are required for replication of viral RNA whereas others are needed for assembly of infectious virus particles. In addition to serving as co-factors during virus replication and assembly, the mechanism by which a given helicase functions in these processes may vary considerably. Moreover, in some cases the enzymatic activity of a helicase may not even be required for its role in the infection pathway. For example, the helicase activity of the NS3 protein is dispensable for its function assembly of infectious yellow fever virions (Patkar and Kuhn, 2008).

In the present study, we investigated the mechanism by which the nucleolar helicase DDX56 functions in morphogenesis of WNV virions. Our data show that inactivating mutations in the DEAD box motif of DDX56 impair its role in production of infectious WNV virions. Similarly, over-expression of the capsid-binding region of DDX56 has a negative impact on WNV infectivity. Together, these findings are consistent with a scenario in which the interaction between catalytically active DDX56 and the WNV capsid protein is an important step during packaging genomic RNA into nascent virions.

Results

Construction of RNAi-resistant DDX56 mutants

As a first step toward determining whether the enzymatic activity of DDX56 is required for infectivity of WNV particles, we constructed DDX56 mutants that lack helicase function. The DEAD box motif is highly conserved in a subgroup of RNA helicases (Schmid and Linder, 1992) and mutagenesis studies have shown that substitution of asparagine for aspartate or glutamine for glutamate results in complete loss of helicase activity (Pause and Sonenberg, 1992). In addition to creating D166N and E167Q mutations in DDX56, silent mutations were introduced downstream of the DEAD box motif in an shRNA target site (Fig. 1). The latter mutations allow the expression of the DEAD box mutants in stable cell lines in which endogenous levels of DDX56 have been reduced by RNA interference (Fig. 2A).

HEK293T cells stably expressing DDX56-specific or non-silencing shRNAs were transduced with lentiviruses encoding AcGFP and myc-tagged wild type DDX56 or DEAD box mutants. Expression of the myc-tagged DDX56 proteins was monitored by immunoblot analyses at 48 h post-transduction. Immunoblot analyses show that compared to expression in non-silencing (NS) cells, the level of wild type myc-tagged DDX56 (WT-RNAi-S) in DDX56 knockdown cells was just on the threshold of detection with the anti-myc antibody (Fig. 2B, lanes 3 and 9). In contrast, the myc-tagged RNAi-resistant forms of wild type DDX56 as well as the D166N and E167Q mutants were robustly expressed in the DDX56 knockdown cells (Fig. 2B, lanes 10–12). These data demonstrate that mutant versions of DDX56 are stable in a cellular background in which endogenous DDX56 is depleted by RNAi.

DEAD box mutants are correctly targeted to the nucleolus

Next, it was important to demonstrate that the DEAD box mutants were correctly targeted to the nucleolus similar to wild type DDX56 (Zirwes et al., 2000). Mock- and WNV-infected A549 cells were transfected with plasmids encoding wild type or DEAD box mutants of DDX56. As evidenced by colocalization with nucleolin, both RNAi-sensitive and -resistant forms of myc-tagged DDX56 are targeted to the nucleoli (Fig. 3). Similarly, the DEAD box mutants D166N and E167Q localized to nuclei of A549 cells. These data confirm that mutations in the DEAD box motif or shRNA targeting sites within the DDX56 open reading frame do not alter targeting of the helicase.

Helicase activity of DDX56 is important for infectivity of WNV

To determine whether enzymatic activity of DDX56 was important for viral gene expression and/or infectivity of WNV, DDX56 knockdown cells expressing RNAi-sensitive or resistant forms of myc-tagged DDX56 proteins were infected with WNV. At 48 h post-infection, cell lysates and supernatants were subjected to immunoblot analyses and plaque assays, respectively. The immunoblot in Fig. 4A shows that based on AcGFP expression, similar levels of transduction efficiency were achieved for all of the DDX56 constructs. As expected, only the RNAi-resistant forms of DDX56 were detected by immunoblotting with anti-myc. In agreement with a recent report from our laboratory (Xu et al., 2011), titers of WNV from DDX56 depleted cells were reduced more than 100 fold compared to those from non-silencing controls (Fig. 4B). However, infection of cells expressing RNAi-resistant DDX56 resulted in normal viral titers, which were well over 1×10^8 pfu/ml. In contrast, infection of cells expressing RNAi-sensitive DDX56 or DEAD box mutants produced viral titers that were similar to DDX56 knockdown cells that had been transduced with a lentivirus encoding AcGFP only. Capsid protein was efficiently co-immunoprecipitated with D166N and E167Q mutants (Fig. 4C) and thus the failure of these DEAD box mutants to complement the production of

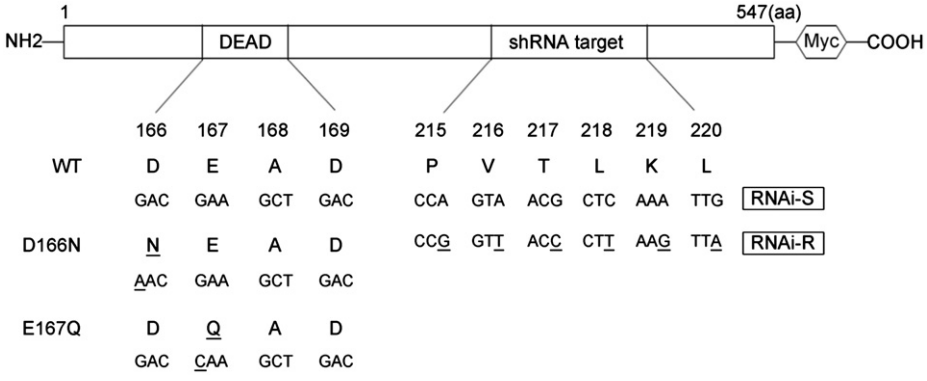

Fig. 1. Construction of RNAi-resistant forms of DDX56 with mutations in the DEAD box motif. Aspartate (D) and glutamate (E) residues in the DEAD box motif of DDX56 were changed to asparagine (N) and glutamine (Q) to produce D166N and E167Q mutants, respectively. In addition, silent mutations were introduced into siRNA-binding sites to make the resulting constructs resistant to RNAi. All constructs contain a myc tag at the C-terminus.

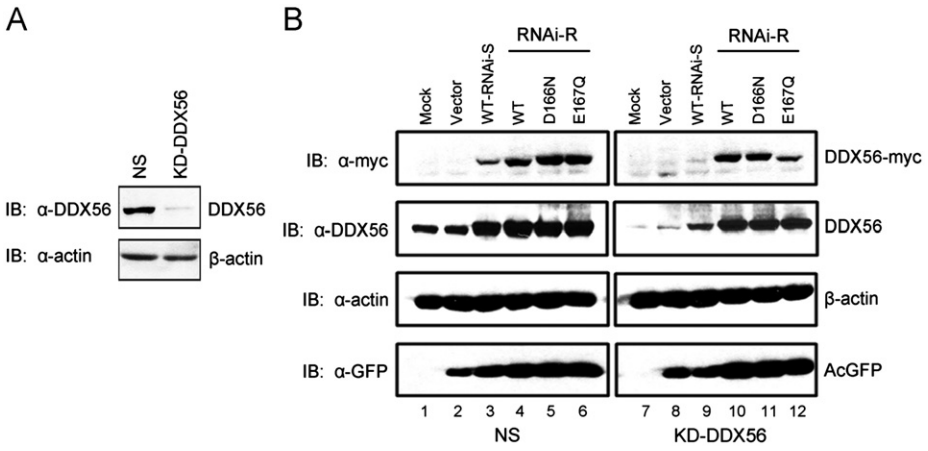

Fig. 2. Expression of RNAi-resistant DDX56 mutants. (A) Immunoblot analyses of DDX56 in stable HEK293T cell lines expressing DDX56-specific (KD-DDX56) or non-silencing (NS) shRNAs. (B) The stable HEK293T cell lines were transduced with lentiviruses encoding normal (RNAi-sensitive) or RNAi-resistant versions of myc-tagged WT and D166N and E167Q mutants. The lentiviruses also encode AcGFP, which is used to monitor transduction of cells. Forty-eight hours post-transduction, levels of endogenous and myc-tagged DDX56 proteins were determined by immunoblotting.

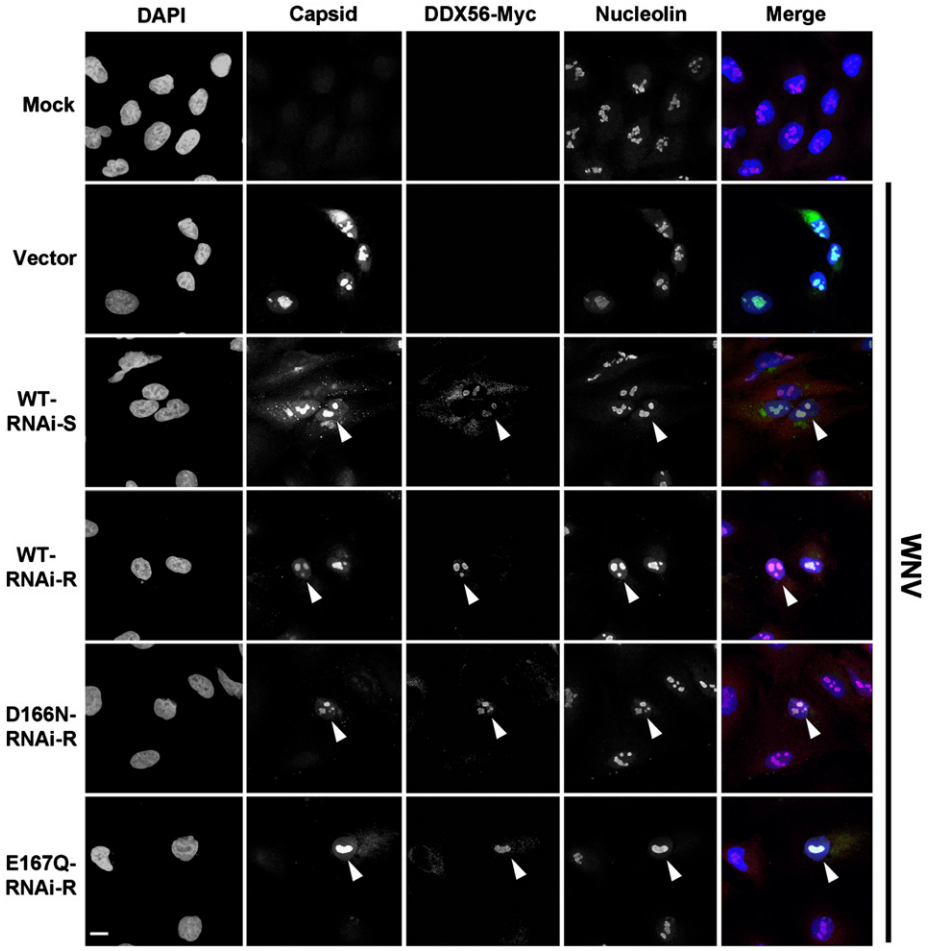

Fig. 3. Mutations in the DEAD box active site of DDX56 do not affect targeting to the nucleolus. A549 cells were transfected with plasmids encoding myc-tagged wild type (WT), D166N, and E167Q mutants as well as a vector. Twenty-four hours post-transfection, cells were infected with WNV (MOI = 5) for 24 h and then fixed and processed for indirect immunofluorescence using mouse anti-myc, rabbit anti-nucleolin, and guinea pig anti-WNV capsid antibodies. Primary antibodies were detected using donkey anti-mouse Alexa546, donkey anti-rabbit Alexa647 and goat anti-guinea pig Alexa488 secondary antibodies. Arrowheads indicate colocalization between capsid, DDX56 proteins and the nucleolar resident protein nucleolin. Nuclei were stained with DAPI. RNAi-sensitive (RNAi-S) and RNAi-resistant (RNAi-R) forms of WT and DDX56 mutants are indicated. Images were captured using a leica TCS SP5 confocal scanning microscope. Size bar = 10 μm.

infectious WNV virions was not due to an inability to bind capsid. Despite the large decrease (> 100-fold) in viral titers, expression of DEAD box mutants did not interfere with replication of WNV. This conclusion is based on the observation that levels of WNV capsid protein were normal in these cells (Fig. 4A).

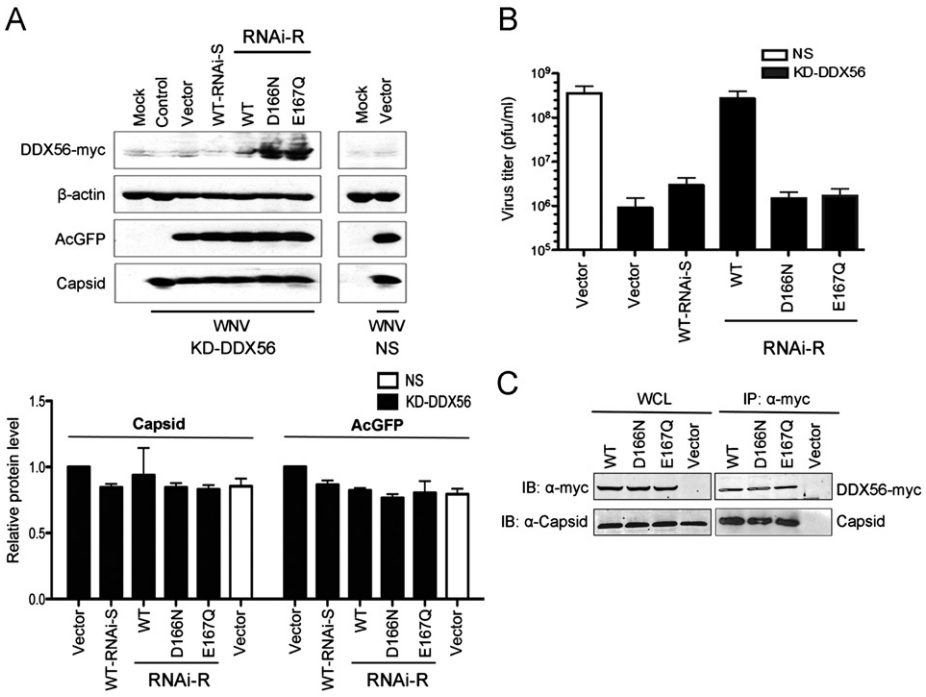

Fig. 4. Helicase activity of DDX56 is important for WNV infectivity. (A) DDX56 knockdown (KD-DDX56) and non-silencing (NS) stable HEK293T cells were transduced with lentiviruses encoding myc-tagged DDX56 constructs that were RNAi resistant (RNAi-R) or sensitive (RNAi-S). Cells were then infected with WNV (MOI=5) and at 48 h cell lysates were analyzed by immunoblotting (upper panel). Relative amounts of capsid and AcGFP (normalized to actin) were quantitated (lower panel). (B) Levels of infectious virus in the conditioned media of the transduced and infected cells were determined by plaque assays. (C) HEK293T cells were transfected with myc-tagged wt and DEAD box mutants of DDX56. At 24 h post-transfection, cells were infected with WNV (MOI=5) for 24 h and then whole-cell lysates (WCL) and mouse anti-myc immunoprecipitates were subjected to SDS-PAGE and immunoblotting with mouse anti-myc or rabbit anti-WNV capsid antibodies.

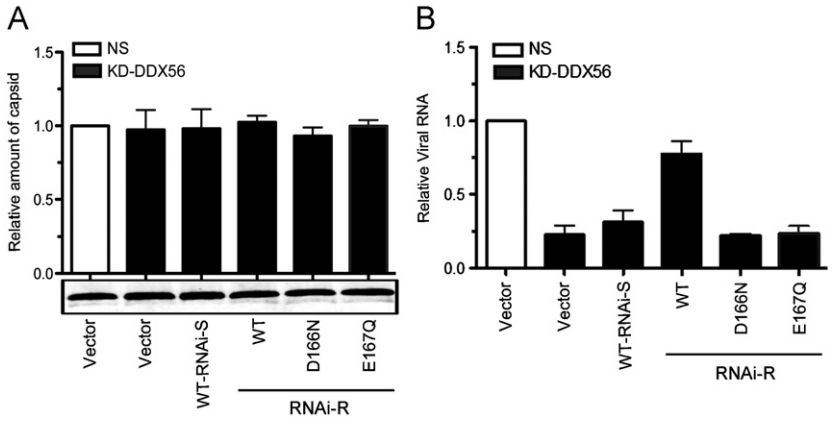

Fig. 5. Helicase activity of DDX56 is important for packaging genomic RNA into WNV particles. (A) WNV virions were recovered from the conditioned media of infected stable DDX56 knockdown (KD-DDX56) and non-silencing control (NS) HEK 293T cells by ultracentrifugation. The crude virion preparations were subjected to SDS-PAGE and immunoblot analyses with rabbit anti-capsid antibody. The relative amounts of capsid from three independent experiments were quantitated. (B) Levels of viral genomic RNA in the virions were determined by RT-PCR. The average relative levels of viral RNA (normalized to capsid protein) from three independent experiments (each conducted in triplicate) were quantitated. Bars indicate standard error values.

Helicase activity of DDX56 is important for packaging viral RNA into virions

Our recent studies suggest that DDX56 may function in packaging viral genomic RNA into nascent virions (Xu et al., 2011). To establish whether the helicase activity of DDX56 is important for this process, we assayed the relative amounts of genomic RNA in WNV particles secreted from cells expressing D166N and E167Q mutants. Loss of DDX56 helicase activity did not affect expression of WNV capsid protein (Fig. 4A) nor its secretion from infected cells in the form of virus particles (Fig. 5A). To determine if packaging of viral RNA was affected, total RNA was extracted from WNV particles and the relative amounts of genomic RNA (normalized to capsid protein) were determined by RT-PCR. Data in Fig. 5B show that virus particles isolated from infected cells expressing helicase dead mutants D166N and E167Q contained 3–4 times less genomic RNA than those isolated from non-silencing cells or cells expressing RNAi-resistant wild type DDX56. These data indicate that the enzymatic activity of DDX56 is important for packaging genomic RNA into WNV virions.

Over-expression of the capsid-binding region of DDX56 reduces infectivity of WNV

The data shown above together with results from our previous study (Xu et al., 2011) are consistent with a scenario in which interaction between WNV and catalytically active DDX56 plays an important role in assembly of infectious virions. If this is indeed the case, blocking interaction between capsid and DDX56 should also reduce the yield of infectious WNV. Our approach was to over-express the capsid-binding region of DDX56 in order to prevent interaction of endogenous DDX56 with capsid. To identify the region of DDX56 that binds to capsid, myc-tagged constructs encoding the N- and C-terminal regions of DDX56 were co-expressed with WNV capsid in transfected cells followed by coimmunoprecipitation and immunoblotting. Data in Fig. 6 show that in transfected or infected cells, the WNV capsid does not bind to the DEAD box helicase-containing region of DDX56 (DDX56-NT-myc), but rather, the C-terminal part of the protein, which was produced in cells expressing DDX56-CT-myc. This region of DDX56 also contains the targeting information that is required for localization to the nucleolus (Fig. 7).

Next, lentiviruses encoding myc-tagged DDX56 N- and C-terminal regions were used to transduce HEK293T cells, which were then infected with WNV. At 48 h post-infection, cell lysates and culture supernatants were subjected to immunoblot and plaque assays, respectively. Data in Fig. 8A show that expression of full length, N- or C-terminal regions of DDX56 do not affect viral gene expression based on the observation that similar levels of capsid protein were detected in all of the infected cell lysates. However, expression of DDX56-CT-myc reduced viral titers approximately 50-fold compared to expression of full length DDX56-myc or NT-DDX56-myc (Fig. 8B). While these results suggest that interaction between WNV capsid and DDX56 is important for a post-replication step in the WNV infection cycle, assembly and secretion of WNV particles was not affected (Fig. 8C). But the fact that significantly less viral RNA was detected in the virus particles is consistent with our hypothesis that capsid-DDX56 interactions are important for incorporation packaging viral genome.

Discussion

Conventional antiviral therapies involve targeting virus-encoded enzymes that are required for replication, processing of polyproteins or viral egress from host cells. While there have been

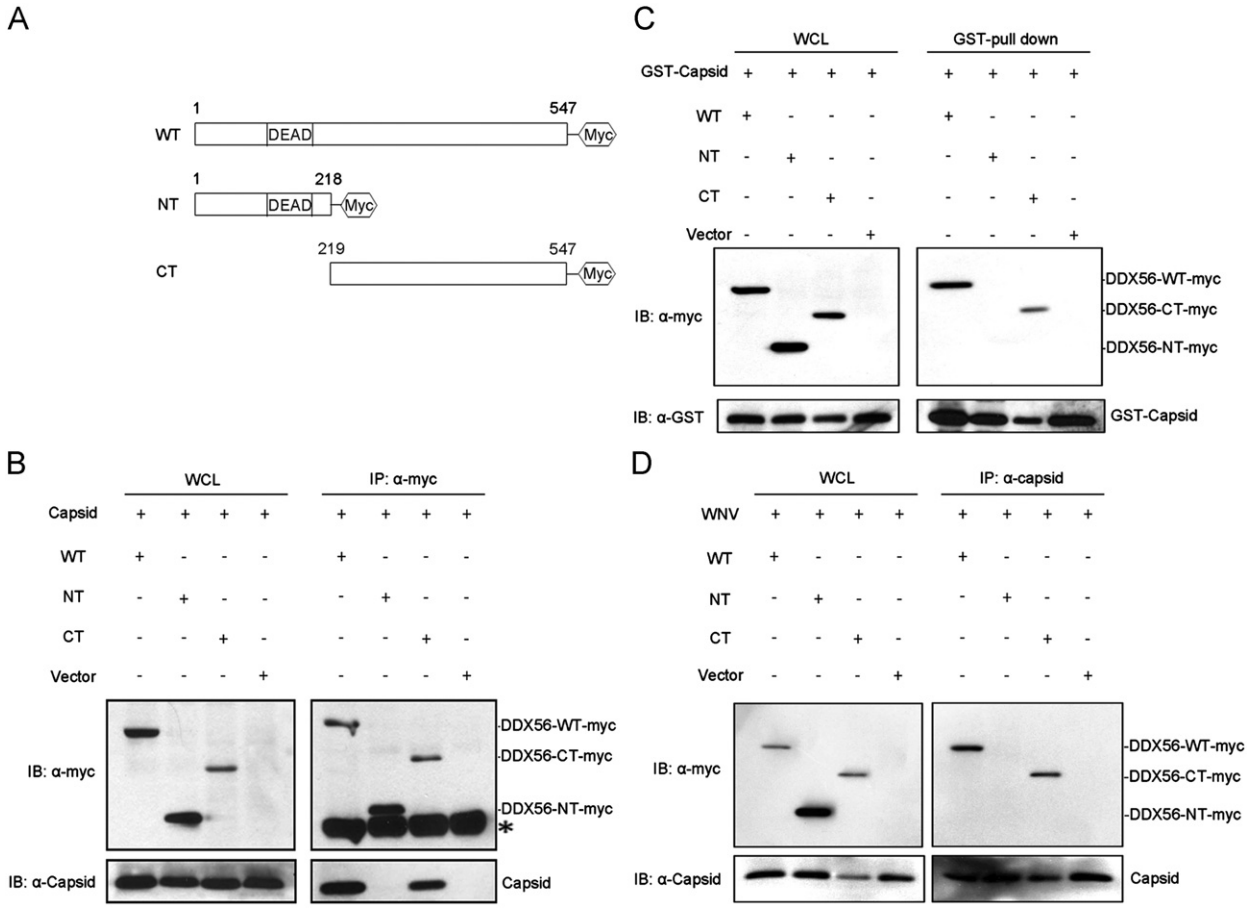

Fig. 6. The C-terminus of DDX56 binds to the WNV capsid protein. (A) Structure and size (amino acid residues) of myc-tagged wild type (WT), N-terminal (NT) and C-terminal (CT) DDX56 constructs. (B) HEK293T cells were co-transfected with plasmids encoding DDX56 constructs with WNV capsid protein. In the left panel, relative levels of myc-tagged DDX56 proteins and capsid were determined in whole cell lysates (WCL) by immunoblotting with antibodies to the myc epitope and WNV capsid protein. In the right panel, cell lysates were subjected to immunoprecipitation followed by immunoblotting with antibodies to myc and capsid. The protein marked by * is IgG light chain. (C) HEK293T cells were co-transfected with plasmids encoding GST-capsid together with WT, NT and CT DDX56 constructs or vector alone. In the left panel, relative levels of myc-tagged DDX56 proteins and capsid were determined in whole cell lysates (WCL) by immunoblotting with antibodies to the myc epitope and GST. In the right panel, cell lysates were subjected to GST-pulldown followed by immunoblotting with antibodies to myc and GST. (D) HEK293T cells were co-transfected with plasmids encoding DDX56 constructs and then infected with WNV. In the left panel, relative levels of myc-tagged DDX56 proteins and capsid were determine in whole cell lysates (WCL) by immunoblotting with antibodies to the myc epitope and WNV capsid protein. In the right panel, cell lysates were subjected to immunoprecipitation by anti-capsid antibody followed by immunoblotting with antibodies to myc and capsid.

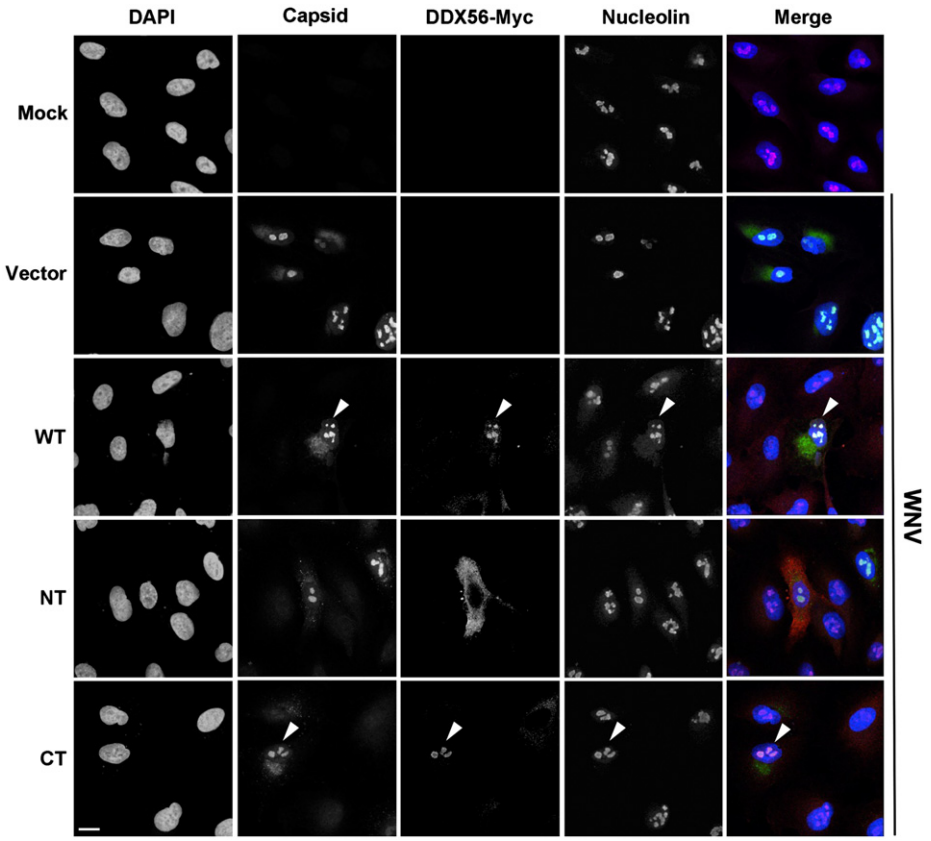

Fig. 7. Nucleolar targeting information of DDX56 is contained in the C-terminal 329 amino acid residues. A549 cells were transfected with plasmids encoding myc-tagged wild type (WT) DDX56, DDX56-NT or DDX56-CT. Twenty-four hours post-transfection, cells were infected with WNV (MOI=5) for 24 h and then fixed and processed for indirect immunofluorescence using mouse anti-myc, rabbit anti-nucleolin, and guinea pig anti-WNV capsid antibodies. Primary antibodies were detected using donkey anti-mouse Alexa546, donkey anti-rabbit Alexa647 and goat anti-guinea pig Alexa488 secondary antibodies. Arrowheads indicate colocalization between capsid, DDX56 constructs and the nucleolar resident protein nucleolin. Nuclei are stained with DAPI. Images were captured using a leica TCS SP5 confocal scanning microscope. Size bar=10 μm.

notable successes using this approach, it suffers from a number of limitations. First, viruses almost invariably develop resistance to these types of drugs. This is particularly true of RNA viruses whose polymerases do not possess proof reading activity and are therefore by nature, error prone and mutable. Second, the choice of targets is very limited due to the small number of enzymes encoded by most viruses. In contrast, targeting host factors as means to control viral infection is a burgeoning area that has shown promise, particularly for flaviviruses. Replication and assembly of infectious flavivirus particles requires hundreds of host genes (Krishnan et al., 2008). Accordingly, it may be possible to target a variety of host proteins, particularly enzymes, as a means to control viral infection. Although this approach may also have drawbacks, viral resistance to small molecules that block host enzymes should be minimal.

RNA helicases are one class of host enzymes that have been proposed as anti-viral targets (Geiss et al., 2009; Kwong et al., 2005; Maga et al., 2011; Stankiewicz-Drogon et al., 2010). Among the helicase superfamily, DEAD box proteins form the largest group of these enzymes. These helicases are thought to play multiple roles in RNA metabolism including mRNA splicing and transport, transcription, translation and remodeling of ribonucleoprotein complexes. In most cases, the physiological substrates of DEAD box helicases have not been defined but it is clear that a number of pathogenic RNA viruses require these enzymes for replication and/or assembly. For example, at least two cellular helicases, DDX1 and DDX3 function as cofactors that promote replication of HIV (Fang et al., 2004; Yedavalli et al., 2004). DDX1 and DDX3 both appear to facilitate export of HIV RNA from the nucleus to the cytoplasm through interaction with Rev. DDX1 also stimulates replication of coronavirus RNA (Xu et al., 2010). However, because coronaviruses replicate in the cytoplasm, it would appear that the role DDX1 plays in replication of these large RNA viruses is distinct from its function as a cofactor for HIV.

Yeast two hybrid and RNA interference screens have also identified DEAD box helicases that play significant roles in the biology of flavivirus infections (Ariumi et al., 2007; Krishnan et al., 2008; Mamiya and Worman, 1999). Many of these enzymes likely function in replication of viral RNA however recent evidence suggests that helicases are needed for efficient virus assembly too. For example, we recently determined that the nucleolar helicase DDX56 is needed for a critical post-replication step in WNV morphogenesis (Xu et al., 2011). DDX56 appears to function in assembly of pre-ribosomal particles, but it is not associated with mature ribosomes (Zirwes et al., 2000). By analogy, it is tempting to speculate that DDX56 functions similarly in assembly of other large ribonucleoprotein particles such as viral nucleocapsids. The fact that DDX56 is not detected in mature WNV virions (Xu et al., 2011) is consistent with this scenario. A related study by another laboratory revealed that DDX24 performs a similar function during assembly of HIV virions (Ma et al., 2008).

DDX56 is not required for viability of cells in vitro (Xu et al., 2011) and therefore, targeting the activity of this enzyme could prove beneficial in controlling WNV and potentially other flavivirus infections. Rather than using RNAi to down-regulate expression of DDX56 in cells, it would be advantageous to use small molecule inhibitors that target the enzymatic activity of this

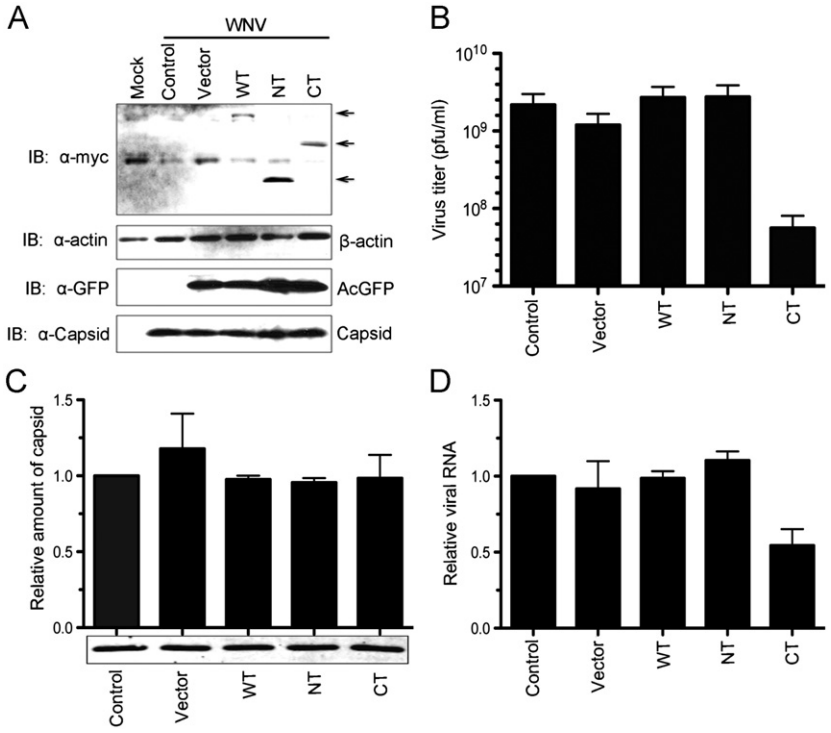

Fig. 8. Expression of the capsid-binding region of DDX56 reduces infectivity of WNV. HEK293T cells were transduced with lentiviruses encoding AcGFP and myc-tagged wild type (WT), N-terminal (NT) and C-terminal (CT) regions of DDX56. The next day, cells were infected with WNV and at 48 h post-infection, cell lysates and culture supernatants were harvested. (A) Immunoblot analyses showing expression of myc-tagged DDX56 constructs (arrows), actin (loading control), AcGFP (transduction efficiency indicator) and WNV capsid protein. Arrowheads indicate the positions of WT, NT and CT DDX56 constructs. (B) Plaque assay was used to determine the titers of WNV secreted from cells transduced with lentiviruses encoding AcGFP alone (vector), WT DDX56, NT or CT constructs. (C) WNV virions secreted from HEK293T cells transduced with lentiviruses encoding AcGFP alone (vector), DDX56 WT, NT or CT constructs were recovered by ultracentrifugation. The crude virion preparations were subjected to SDS-PAGE and immunoblot analyses with rabbit anti-capsid antibody. The relative amounts of capsid from three independent experiments were quantitated (A). (D) Levels of viral genomic RNA in the virions were determined by RT-PCR. The average relative levels of viral RNA (normalized to capsid protein) from three independent experiments (each conducted in triplicate) were quantitated. Bars indicate standard error values.

protein. If this is to be a feasible approach, it was important to demonstrate that the helicase activity of DDX56 is in fact required for its role in WNV infectivity. While this may seem intuitive, the enzymatic function of a "helicase" is not always required for its role in virus biology. Indeed, among highly related viral helicases, the mode of action during virus assembly can vary greatly. For example, assembly of infectious Kunjin virus, a close relative of WNV, requires expression of the viral NS3 protein in *cis* (Liu et al., 2002). In contrast, during assembly of yellow fever virus particles, the helicase activity of NS3 is not required for this process (Patkar and Kuhn, 2008). Moreover, yellow fever virus NS3 can perform its virus assembly function when expressed in *trans* unlike Kunjin virus NS3 which must be expressed in *cis*.

The helicase activity of DDX56 is not essential for replication or assembly of WNV virions per se but our data indicate that it is critical for infectivity of virus particles. Moreover, because over-expression of the capsid-binding region of DDX56 has a similar effect as reducing expression of DDX56 or knocking out its helicase activity, we hypothesize that interaction between capsid and this host enzyme facilitate loading and/or organization of viral RNA during virus assembly. Through an unknown mechanism, WNV infection causes relocalization of DDX56 from the nucleolus to cytoplasmic structures that are enriched in capsid protein (Xu et al., 2011). It is likely that these capsid-positive cytoplasmic elements are virus assembly sites on the endoplasmic reticulum. Next, it will be of interest to develop small molecule inhibitors that can be used to target the helicase activity of DDX56. These inhibitors would not be expected to block replication of WNV, but by reducing the infectivity of nascent virions, viral spread would be minimized thereby allowing the immune system to contain the infection.

Materials and methods

General lab reagents

Laboratory reagents were purchased from the following sources: Complete™ EDTA-free protease inhibitor cocktail from Roche Diagnostics (Laval, Quebec); Protein G-sepharose from GE Healthcare Bio-Sciences AB (Piscataway, NJ); Per-Fectin transfection reagent from Genlantis (San Diego, CA); TransIT®-293 transfection regent from MirusBio (Madison, WI); Pierce BCA Protein Assay Kit from Thermo Scientific (Rockford, IL); human full-length verified DDX56 cDNA (Clone id 3456547) and human GIPZ lentiviral shRNAmir individual clone (Clone id V3LHS_353980) targeting DDX56 mRNA from Open Biosystems (Huntsville, AL); HEK 293T, A549 and BHK21 cells from the American Type Culture Collection (Manassas, VA); PerfeCTa™ SYBR® Green Supermix Low ROX from Quanta Biosciences (Gaithersville, MD); SuperScript III reverse transcriptase cDNA synthesis kit, random primers, ProLong® Gold Anti-fade reagent with 4′-6-diamidino-2-phenylindole (DAPI) and all other reagents for mammalian cell culture were obtained from Invitrogen (Carlsbad, CA).

Antibodies

Antibodies were obtained from the following sources: DDX56-specific mouse monoclonal from PROGEN Biotechnik (Heidelberg, Germany); rabbit and guinea pig polyclonal antibodies to WNV capsid protein were generated in this laboratory (Hunt et al., 2007; Xu et al., 2012); myc-specific mouse monoclonal antibodies were purified from 9E10 hybridoma cells from ATCC (Manassas, VA);

β-actin-specific mouse monoclonal antibody, GST-specific rabbit polyclonal antibody and nucleolin-specific rabbit antibodies from Abcam (Cambridge, MA); green fluorescent protein (GFP)-specific rabbit polyclonal antibody from Dr. L. Berthiaume (University of Alberta, Edmonton, Canada); goat anti-rabbit and goat anti-mouse IgG conjugated to horseradish peroxidase from Jackson Immuno-Research Laboratories (West Grove, PA); donkey anti-mouse IgG conjugated to Alexa Fluor 546, donkey anti-rabbit IgG conjugated to Alexa Fluor 647 and goat anti-guinea pig IgG conjugated to Alexa Fluor 488 from Invitrogen (Carlsbad, CA).

Plasmids

All plasmids were constructed using PCR and standard sub-cloning techniques. Prior to use in experiments, the newly constructed plasmids were verified by diagnostic restriction endonuclease digestion and DNA sequencing.

RNAi-resistant and DEAD box mutants of DDX56

Constructs encoding myc-tagged RNAi resistant forms of DDX56 were generated using the overlap extension PCR method. For the first PCR, the plasmid pcDNA3.1(-)-DDX56-myc (Xu, Anderson, and Hobman, 2011) served as the template. Primer pairs used for the first PCR were NotI-F and RNAi-resistant-R and MluI-R and RNAi-resistant-F (Table 1). The RNAi-resistant mutations were designed based on the target sequence recognized by the DDX56-specific shRNAmir-353980 targeting sequence as shown in Fig. 1. The product of the overlap PCR which was amplified using primers NotI-F and MluI-R was subcloned into the Not I and Mlu I sites of pLVX-Tight-Puro to produce pLVX-DDX56-wt-RNAi-R. To generate RNAi-resistant DEAD box mutants of DDX56, the wild type RNAi resistant DDX56 cDNA produced as described above was subjected to PCR using the primer pair NotI-F/MluI-R together with primers that introduce mutations into the DEAD box motif (D166N-F and D166N-R; E167Q-F and E167Q-R). The resulting cDNAs (D166N and E167Q) were then subcloned into the Not I and Mlu I sites of pLVX-Tight-Puro to produce pLVX-DDX56-D166N-RNAi-R and pLVX-DDX56-E167Q-RNAi-R, respectively.

The cDNAs encoding RNAi-resistant wild type, D166N and E167Q DDX56 were excised from the pLVX plasmids and sub-cloned into the Spe I and Xho I sites of the lentiviral vector pTRIP-CMV-MCS-IRES-AcGFP. The resulting plasmids pTRIP-AcGFP-DDX56-wt, D166N, and E167Q-RNAi-R, respectively, direct independent expression of AcGFP and DDX56 wild type and mutants. The plasmid pTRIP-AcGFP-DDX56-wt-RNAi-S (sensitive) was created by ligation of a cDNA encoding wild type myc-tagged DDX56 into the Spe I and Xho I sites of pTRIP-IRES-AcGFP.

Deletion mutants of DDX56

DNA fragments encoding myc-tagged amino acid residues 1–218 and 219–547 of DDX56 were generated by PCR with primers pairs DDX56-F/DDX56-NT-R and DDX56-CT-F/DDX56-R, respectively, using the plasmid pcDNA3.1(-)-DDX56-myc (Xu, Anderson, and Hobman, 2011) as template. The resulting cDNAs were ligated into the EcoR I and BamH I sites of the mammalian expression vector pcDNA3.1(-)-myc. Myc-tagged DDX56-NT and DDX56-CT cDNAs produced by PCR using primers SpeI-EcoRV-F and XhoI-R were also ligated into the Spe I and Xho I sites of the lentiviral vector pTRIP-CMV-MCS-IRES-AcGFP.

Construction of the mammalian expression plasmid encoding the 105 amino acid isoform of WNV capsid, pCMV5-Capsid, has been described previously (Hunt et al., 2007).

Cell culture and transfection

HEK293T and A549 cells were cultured in DMEM supplemented with 100 U/ml penicillin/streptomycin, 10% heat-inactivated fetal bovine serum and 10 mM HEPES, pH 7.4, at 37 °C and 5% CO_2. DNA transfections were performed using Perfectin or TransIT®-293 transfection reagent as described by the manufacturers.

Indirect immunofluorescence

A549 cells grown on coverslips were transfected with plasmids encoding myc-tagged full length and truncation DDX56 constructs. At 24 h post-transfection, cells were infected with WNV (MOI=5) for 24 h and then fixed and processed for indirect immunofluorescence microscopy. Coverslips were mounted onto microscope slides using ProLong Gold antifade reagent with DAPI, after which the samples were examined using a Leica TCS SP5 confocal microscope. In all cases, samples were viewed using 63× objective lens and images were acquired using identical

Table 1
Oligonucleotide primers.

Primer name	Sequence	Restriction enzyme site	Usage
NotI-F	5-ACT CGA GCG GCCGCC ACT GTG CTG GAT ATC-3	Not I	Cloning
MluI-R	5-GCGTACGCGTTCACAGATCCTCTTCTGAGATGAG-3	Mlu I	Cloning
RNAi resistant-F	5-GCTGATATTACATAACCCAGTAACGCTCAAATTGCAGGA GTCCCAGCTGCCTG-3		Cloning
RNAi resistant-R	5-CAGGCAGCTGGGACTCCTGCAATTTGAGCGTTACTGGGTT ATGTAATATCAGC-3		Cloning
D166N-F	5-GCTTTTGGTGGTGAACGAAGCTGACC-3		Cloning
D166N-R	5-GGTCAGCTTCGTTCACCACCAAAAGC-3		Cloning
E167Q-F	5-CTTTTGGTGGTGGACCAAGCTGACCTTC-3		Cloning
E167Q-R	5-GAAGGTCAGCTTGGTCCACCACCAAAAG-3		Cloning
SpeI-F	5-CTAT ACTAGTCCGCCACCATGGAGGACTCTG-3	Spe I	Cloning
XhoI-R	5-CGGT CTCGAG TCA CAG ATC CTC TTC TGA G-3	Xho I	Cloning
SpeI-EcoRV-F	5-CTAT ACTAGT ACT GTG CTG GAT ATC TGC AG-3	SpeI, EcoR V	Cloning
DDX56-F	5-CTATGAATTCGCCACCATGGAGGACTCTGAAGCACTG-3	EcoR I	Cloning
DDX56-R	5-GCGTGGATCCGGAGGGCTTGGCTGTGGGTCTG-3	BamH I	Cloning
NT-R	5-GCGT GGA TCC AAG GGT AAC CGG GTT ATG TAA-3	BamH I	Cloning
CT-F	5-CTATGAATTCGCCACCATGAAGTTACAGGAGTCCCAG-3	EcoR I	Cloning
WNV-env-F	5-TCA GCG ATC TCT CCA CCA AAG-3		qRT-PCR
WNV-env-R	5-GGG TCA GCA CGT TTG TCA TTG-3		qRT-PCR
Cyclophilin-F	5-TCC AAA GAC AGC AGA AAA CTT TCG-3		qRT-PCR
Cyclophilin-R	5-TCT TCT TGC TGG TCT TGC CAT TCC-3		qRT-PCR

exposure times for each channel. Images were processed using Image J and LAS AF Lite software.

Coimmunoprecipitation and GST pull-down

HEK293T cells (1.2×10^6) were seeded into 100-mm-diameter dishes and the next day, were transfected with expression plasmids (8 μg) using PerFectin. After 48 h, cells were washed with phosphate-buffered saline (PBS) and then lysed with NP-40 lysis buffer (150 mM NaCl, 2 mM EDTA, 1% non-idet P-40, 50 mM Tris–HCl [pH 7.2], 1 mM fresh dithiothreitol) containing protease inhibitors on ice for 30 min. Lysates were clarified by centrifugation for 10 min at 14,000 rpm in a microcentrifuge at 4 °C. Small aliquots of the clarified lysates were kept for loading controls. The remaining lysates were precleared with Protein A- or G-Sepharose beads for 1 h at 4 °C before sequential incubation with mouse anti-myc antibodies for 3 h and then Protein A- or G-Sepharose beads for 2 h at 4 °C. For the GST pull-down experiments, cleared lysates were incubated with glutathione-Sepharose 4B beads for 2 h at 4 °C. Immunoprecipitates and GST pull-downs were washed three times with lysis buffer before the bound proteins were eluted by boiling in protein sample buffer. Proteins were separated by SDS-PAGE and transferred to polyvinylidene difluoride membranes for immunoblotting.

Stable knockdown of DDX56 in HEK293T cells

Stable HEK293T cell lines expressing a DDX56-specific (Clone id V3LHS_353980 Open Biosystems) or a non-silencing shRNAmir (catalog number RHS4346; Open Biosystems) were created by lentiviral transduction followed by puromycin selection (1 μg/ml) as described (Xu et al., 2011). After selection, the resulting polyclonal cell lines were maintained in media containing 0.25 μg/ml puromycin.

Production of lentiviruses for expression of DDX56 mutants

HEK293T cells (2.5×10^6) in 100 mm dishes were co-transfected with pTRIP-AcGFP plasmids encoding myc-tagged DDX56 cDNAs (WT, D166N, E167Q, NT or CT), pGag-Pol (5.6 μg) and pHCMV-VSVG (1.6 μg) using TransIT®-293 transfection reagent. Forty-eight hours later, polybrene (4 μg/ml) and HEPES (20 mM) were added to the lentivirus-containing culture supernatants which were then passed through 0.45 μm filter before aliquotting. Stocks were stored at −80 °C or used immediately to transduce HEK293T or A549 cells. Typically, lentiviral stocks were diluted 1:10 in DMEM containing 3% FBS, polybrene (4 μg/ml) and HEPES (20 mM). Cells were then spinoculated by centrifugation at 1200 rpm in an Eppendorf A-4-62 rotor for 1 h at 37 °C after which the plates were transferred to a 37 °C incubator. After 6 h, the media were replaced with DMEM containing 10% FBS. Unless otherwise indicated, transduced cells were analyzed 48 h post-transduction.

WNV infection

WNV strain NY99 was kindly provided by Mike Drebot (Public Health Agency of Canada, Winnipeg, MB). All virus manipulations were performed under level 3 containment conditions. Unless otherwise indicated, cultured cells were infected using an MOI of 5. Plaque assays were conducted using BHK21 cells as described (Xu et al., 2011).

To recover WNV particles from infected cells, medium from infected cells was precleared of cell debris by centrifugation for 10 min at 2500 × *g*, after which the resulting supernatants were passed through 0.45-μm filters. Virus was inactivated by exposure to ultraviolet light in a biosafety cabinet for 1 h prior to removal of the material out of the level 3 facility. WNV virions were then recovered from the clarified medium by centrifugation at 100,000 × *g* for 1 h.

Quantitative PCR analysis of viral RNA

Total RNA from crude WNV virion preparations was isolated with TRIzol® reagent (Invitrogen) according to the manufacturer's instructions. Reverse transcription and quantitative PCR analyses of WNV genomic RNA was performed as described (Xu et al., 2011). The relative amount of WNV genomic RNA in each sample was normalized to the amount of capsid protein which was determined by immunoblotting.

Acknowledgments

We thank Eileen Reklow and Valeria Mancinelli for technical support. Z.X. is the recipient of a graduate studentship award from Alberta Innovates Health Solutions (AIHS). T.C.H. holds a Scientist award from AIHS and is a Canada Research Chair. This work was supported by operating funds from the Canadian Institutes of Health Research.

References

Ariumi, Y., Kuroki, M., Abe, K., Dansako, H., Ikeda, M., Wakita, T., Kato, N., 2007. DDX3 DEAD-box RNA helicase is required for hepatitis C virus RNA replication. J. Virol. 81 (24), 13922–13926.

Brinton, M.A., 2002. The molecular biology of West Nile virus: a new invader of the western hemisphere. Annu. Rev. Microbiol. 56, 371–402.

Fang, J., Kubota, S., Yang, B., Zhou, N., Zhang, H., Godbout, R., Pomerantz, R.J., 2004. A DEAD box protein facilitates HIV-1 replication as a cellular co-factor of Rev. Virology 330 (2), 471–480.

Geiss, B.J., Stahla, H., Hannah, A.M., Gari, A.M., Keenan, S.M., 2009. Focus on flaviviruses: current and future drug targets. Future Med. Chem. 1 (2), 327–344.

Hunt, T.A., Urbanowski, M.D., Kakani, K., Law, L.M., Brinton, M.A., Hobman, T.C., 2007. Interactions between the West Nile virus capsid protein and the host cell-encoded phosphatase inhibitor, I2PP2A. Cell Microbiol. 9 (11), 2756–2766.

Krishnan, M.N., Ng, A., Sukumaran, B., Gilfoy, F.D., Uchil, P.D., Sultana, H., Brass, A.L., Adametz, R., Tsui, M., Qian, F., Montgomery, R.R., Lev, S., Mason, P.W., Koski, R.A., Elledge, S.J., Xavier, R.J., Agaisse, H., Fikrig, E., 2008. RNA interference screen for human genes associated with West Nile virus infection. Nature 455 (7210), 242–245.

Kwong, A.D., Rao, B.G., Jeang, K.T., 2005. Viral and cellular RNA helicases as antiviral targets. Nat. Rev. Drug Discov. 4 (10), 845–853.

Liu, W.J., Sedlak, P.L., Kondratieva, N., Khromykh, A.A., 2002. Complementation analysis of the flavivirus Kunjin NS3 and NS5 proteins defines the minimal regions essential for formation of a replication complex and shows a requirement of NS3 in *cis* for virus assembly. J. Virol. 76 (21), 10766–10775.

Ma, J., Rong, L., Zhou, Y., Roy, B.B., Lu, J., Abrahamyan, L., Mouland, A.J., Pan, Q., Liang, C., 2008. The requirement of the DEAD-box protein DDX24 for the packaging of human immunodeficiency virus type 1 RNA. Virology 375 (1), 253–264.

Maga, G., Falchi, F., Radi, M., Botta, L., Casaluce, G., Bernardini, M., Irannejad, H., Manetti, F., Garbelli, A., Samuele, A., Zanoli, S., Este, J.A., Gonzalez, E., Zucca, E., Paolucci, S., Baldanti, F., De Rijck, J., Debyser, Z., Botta, M., 2011. Toward the discovery of novel anti-HIV drugs. Second-generation inhibitors of the cellular ATPase DDX3 with improved anti-HIV activity: synthesis, structure-activity relationship analysis, cytotoxicity studies, and target validation. Chem Med-Chem 6 (8), 1371–1389.

Mamiya, N., Worman, H.J., 1999. Hepatitis C virus core protein binds to a DEAD box RNA helicase. J. Biol. Chem. 274 (22), 15751–15756.

Owsianka, A.M., Patel, A.H., 1999. Hepatitis C virus core protein interacts with a human DEAD box protein DDX3. Virology 257 (2), 330–340.

Patkar, C.G., Kuhn, R.J., 2008. Yellow Fever virus NS3 plays an essential role in virus assembly independent of its known enzymatic functions. J. Virol. 82 (7), 3342–3352.

Pause, A., Sonenberg, N., 1992. Mutational analysis of a DEAD box RNA helicase: the mammalian translation initiation factor eIF-4A. EMBO J. 11 (7), 2643–2654.

Schmid, S.R., Linder, P., 1992. D-E-A-D protein family of putative RNA helicases. Mol. Microbiol. 6 (3), 283–291.

Stankiewicz-Drogon, A., Dorner, B., Erker, T., Boguszewska-Chachulska, A.M., 2010. Synthesis of new acridone derivatives, inhibitors of NS3 helicase, which

efficiently and specifically inhibit subgenomic HCV replication. J. Med. Chem. 53 (8), 3117–3126.
van Marle, G., Antony, J., Ostermann, H., Dunham, C., Hunt, T., Halliday, W., Maingat, F., Urbanowski, M.D., Hobman, T., Peeling, J., Power, C., 2007. West Nile virus-induced neuroinflammation: glial infection and capsid protein-mediated neurovirulence. J. Virol. 81 (20), 10933–10949.
Xu, L., Khadijah, S., Fang, S., Wang, L., Tay, F.P., Liu, D.X., 2010. The cellular RNA helicase DDX1 interacts with coronavirus nonstructural protein 14 and enhances viral replication. J. Virol.
Xu, Z., Anderson, R., Hobman, T.C., 2011. The capsid-binding nucleolar helicase DDX56 is important for infectivity of West Nile virus. J. Virol. 85 (11), 5571–5580.
Xu, Z., Waeckerlin, R., Urbanowski, M.D., van Marle, G., Hobman, T.C., 2012. West Nile virus infection causes endocytosis of a specific subset of tight junction membrane proteins. PLoS One 7 (5), e37886.
Yedavalli, V.S., Neuveut, C., Chi, Y.H., Kleiman, L., Jeang, K.T., 2004. Requirement of DDX3 DEAD box RNA helicase for HIV-1 Rev-RRE export function. Cell 119 (3), 381–392.
You, L.R., Chen, C.M., Lee, Y.H.W., 1999. Hepatitis C virus core protein enhances NF-kappaB signal pathway triggering by lymphotoxin-beta receptor ligand and tumor necrosis factor alpha. J. Virol. 73 (2), 1672–1681.
Zirwes, R.F., Eilbracht, J., Kneissel, S., Schmidt-Zachmann, M.S., 2000. A novel helicase-type protein in the nucleolus: protein NOH61. Mol. Biol. Cell 11 (4), 1153–1167.